Transition in collective motion decision making

Biao Wang,[1] Yue Wu [ORCID],[1] Guangwei Wang [ORCID],[1] Lan Liu,[3,*] Guanrong Chen,[2,†] and Hai-Tao Zhang [ORCID][1,‡]

[1]*School of Artificial Intelligence and Automation, Key Laboratory of Image Processing and Intelligent Control, State Key Laboratory of Digital Manufacturing Equipment and Technology, Huazhong University of Science and Technology, Wuhan 430074, China*
[2]*Department of Electrical Engineering, City University of Hong Kong, Hong Kong SAR, China*
[3]*National Engineering Laboratory for Educational Big Data, Central China Normal University, Wuhan 430079, China*

Collective decision making in a biological motion group requires fast and robust transmission of information. Typically, directional switching information propagation across the whole group obeys a linear dispersion law. However, conventional dynamic collective motion models, such as the Vicsek model and the Couzin model did not take into account ultrafast directional synchronous motions. In the present paper, a multiparticle model is proposed based on inertial spin self-propel action, which can provide adequate description of such group motion. By considering both spin mechanism and collision avoidance, the proposed self-propelled particle spin model can nicely describe collective motion with fast directional switching. By analyzing the order parameter of the group-velocity synchronization, a mechanism of group decision making is revealed, which is based on the difference between two clusters of divergent leaders, showing a transition from the compromising phase (i.e., following the group average) to the preferred phase (i.e., aligning to a leader cluster). The finding provides new insight to the decision-making process of followers when they face with divergent leaders in group motion.

I. INTRODUCTION

Recently, the research topic of collective motions of natural self-propelled entities, referred to as particles hereafter has attracted wide attentions from biologists [1,2], physicists [3–5], systems scientists [6], and control theorists [7,8]. One reason is that different types of group behaviors are ubiquitous in nature, such as bird flocks [9,10], human crowds [11,12], fish schools [13,14], mammal herds [15], bacteria, and cell colonies [16,17]. Particularly, biological particles survive through coordination and collaboration, for instance, cattle gathering to resist enemy attacks and bird flocking to complete long-distance migration. The seemingly low-intelligent individuals with simple mutual interactions can accomplish many complex missions. Today, artificial intelligence systems have learned and benefited a lot from such swarm synergy motions, including collective formation control of drones [18], sensor network data fusion [19], cooperative operation of multirobot teams [20], etc.

The diverse collective patterns generated by self-propelled particles highly depend on interparticle interactions. In the past couple of decades, some dynamic models were proposed to describe such complex collective behaviors. Reynolds [1] introduced a simulation-based model by recording the path of each bird to describe birds flocking. His Boids model can realize the behaviors of biological flocks or swarms according to three heuristic rules: (i) Collision avoidance: Each

simulated particle avoids collision with nearby particles; (ii) velocity matching: each particle matches the average speed of nearby particles to maintain consistency of motion; (iii) flock centering: each particle moves as close as possible to nearby particles. Vicsek *et al.* [3] then proposed a self-propelled particle model, known as the Vicsek model today. Particles in the Vicsek model are driven with a constant speed but with different headings, which results in a kinetic transition from a disordered state to an ordered one of the group with increasing particle density or decreasing external noise intensity. Subsequently, by considering both interparticle attraction and repulsion, Couzin *et al.* [2] established a three-sphere model to study the spatial dynamics of animal groups, such as fish schooling and birds flocking, which can reproduce three typical collective patterns, i.e., flocking, torusing, and swarming. Later, Olfati-Saber [21] suggested an interparticle attraction-repulsion-based dynamic model, which can generate an α-lattice collective migration with obstacle avoidance. Caprini *et al.* have studied a system composed of purely repulsive spherical self-propelled particles and discovered spontaneous velocity alignment phenomenon in motility-induced phase separation [22]. Following this research line, they further revealed the role of the hidden velocity ordering in forming of dense suspension in self-propelled disks [23]. Singh and Rabin [24] built a boundary-driven dynamical model where each particle moves towards the farthest particle, resulting in a certain kinetic pattern of assembly along a line. Furthermore, Vicsek and Zafeiris [25] proposed a minimal multiagent system model according to relative distances between particles. Cucker and Smale [26] developed a model in both discrete- and continuous-time domains, taking into account the interactions of particles associated with

*Corresponding author: lanliu@ccnu.edu.cn
†Corresponding author: eegchen@cityu.edu.hk
‡Corresponding author: zht@mail.hust.edu.cn

their spatial distances. Caprini and Marconi [27] and Szamel and Flenner [28] investigated velocity correlations in self-propelled particle systems. With the assistance of the minimal model [25], Cheng *et al.* [29] showed the pattern transition among four typical collective motion phases, i.e., crystal-like, liquidlike, gaslike, and mill-liquid coexistence patterns. Chen and Zhang [7], and Zhang and co-workers [30–32], discovered a forming mechanism of collective circular motion for self-propelled particle systems, thereby proposing some predictive consensus protocols.

On the other hand, with the tremendous development of sensor hardware technology, a great deal of effort has been devoted to measuring the collective movements of a large group of biological self-propelled particles. By using high-resolution GPS devices, Nagy *et al.* [33] obtained real-time data from tracks of a dozen of homing pigeons flying in flock and proposed a hierarchical communication network model. Through high-speed cameras to film starlings, Attananasi *et al.* [34] measured how information is transmitted through a flock of starlings, which is found analogous to the behavior of a certain quantum phenomenon of liquid helium. As a result, Cavagna *et al.* [35] proposed a self-propelled particle model, which can more vividly describe the linear undamped propagation mechanism of information flows in a starling flock than the popular Vicsek model.

Motivated by the above observations, through extracting some essential factors influencing collective motions, this paper establishes a self-propelled particle model taking into account both moving direction alignment and collision avoidance. By enlarging the divergence of preferred moving directions of two leader clusters, an appealing transition phenomenon of the mass followers' collective moving direction has been found. The present paper sheds some light onto the investigation of decision-making mechanisms for followers with divergent leaders in group motions and helps refine our understanding of the effective leadership of individuals due to their swift information transmission abilities.

II. THE SELF-PROPELLED PARTICLE MODEL

In the current research on the collective behavioral characteristics of biological groups, most models assume that particles in the group make decision based on limited local information, e.g., the Vicsek model [3]. Therein, the instant individual velocity is calculated as

$$\mathbf{v}_i(t + \Delta t) = \rho \left[\sum_{j \in \mathcal{N}_i} \mathbf{v}_j(t) \right] + \Delta \mathbf{v}_i(t), \quad (1)$$

where $\mathbf{v}_i$, $\mathcal{N}_i$, and $\Delta \mathbf{v}_i$ denote the velocity, the neighborhood, and the noise of particle i, respectively; Δt is the sampling period, and $\rho(*) := */\| * \|$ is the normalization of a vector $*$, $i = 1, 2, \dots, N$.

Note that with different velocity-aligned updating rules a multiparticle system can have various collective behaviors [2,3,36]. However, it is observed that the information field intensity in whole starling flocks is undamped at all [34] whereas in the Vicsek model the field keeps decreasing along the information transmission route. Hence, according to conservation law and the spontaneous symmetry breaking

theory, Cavagna *et al.* [35] proposed the following novel continuous-time inertial spin model:

$$\frac{d\vec{v}_i}{dt} = \frac{1}{\chi} \vec{s}_i \times \vec{v}_i,$$

$$\frac{d\vec{s}_i}{dt} = \vec{v}_i(t) \left[v_0^2 \sum_j n_{ij} \vec{v}_j - \frac{\eta}{v_0^2} \frac{d\vec{v}_i}{dt} + \frac{\vec{\xi}_i}{v_0} \right], \quad (2)$$

$$\frac{d\vec{r}_i}{dt} = \vec{v}_i(t),$$

with external noise correlation,

$$\langle \vec{\xi}_i(t) \cdot \vec{\xi}_j(t') \rangle = (2d)\eta T \delta_{ij} \delta(t - t'). \quad (3)$$

In this model, $\vec{r}_i$ is the position of particle i; $\vec{v}_i$ is the velocity (with a constant speed $|\vec{v}_i| = v_0$); $\vec{s}_i$ is the spin of each particle, which represents a generalized momentum, connected to the instantaneous curvature of the particle's trajectory; χ is a generalized moment of inertia; η is a damping coefficient; T is a generalized temperature; J is the strength of the alignment force to neighbors. Moreover, the connectivity matrix n_{ij} describes the neighboring relationship, i.e., $n_{ij} = 1$ means that j is a neighbor of i whereas $n_{ij} = 0$ means not.

It is noted that, in the spin model (2), parameter η plays an indispensable role in tuning the interparticle information transmission. More precisely, a sufficiently small parameter η means low damping, which yields fast and robust information propagation through the entire group, whereas a sufficiently large η implies attenuated information propagation.

The spin model (2) incorporates the physical concept of spin into a dynamical model of bird flocks, which well describes the information transmission between starling flocks [34]. Inspired by this different continuous-time spin model (2), a discrete-time spin model is proposed hereby for numerical studies. By omitting the noise term $\vec{v}_i(t) \times \frac{\vec{\xi}_i}{v_0}$ of the spin time-evolution equation (relatively low Gaussian noise will be added later), it results in

$$\mathbf{s}_i(t + \Delta t) = \mathbf{s}_i(t) e^{-(\lambda \Delta t)} + \mathbf{v}_i(t) \mu \Sigma_j n_{ij} \mathbf{v}_j(t) \Delta t. \quad (4)$$

Here, the damping coefficient η, the generalized moment of inertia χ, and the strength of alignment force J are absorbed into parameters $\lambda := \eta/\chi$ and $\mu := J/v_0^2$, respectively.

As shown in Fig. 1, the vector spin is always perpendicular to the velocity plane, implying that the spin serves as a rotator in changing the direction of the velocity. The first equation about velocity in model (2) is an infinitesimal rotation that leads to tiny finite rotations of velocity when it is simulated with a short time interval.

Then, in the proposed spin model, the equation of velocity is transformed to the following form:

$$\mathbf{v}_i(t + \Delta t) = \rho\{\mathcal{R}[\mathbf{v}_i(t), \kappa s_i(t) \Delta t]\}, \quad (5)$$

where $\kappa = 1/\chi$ is a constant and $\mathcal{R}[\mathbf{v}, \theta]$ denotes the vector $\mathbf{v}$ rotated by $\theta°$. In addition, the collision probability between particles is taken into account to tune their kinetics on the basis of the spin models (4) and (5).

Now, by considering local neighbors, a group of N particles is examined where each particle is described by a position vector $\mathbf{x}_i(t)$, a speed vector $\mathbf{v}_i(t)$ (with a constant speed $|\mathbf{v}_i(t)| = v_0$), and a spin vector $\mathbf{s}_i(t)$.

(a)

(b)
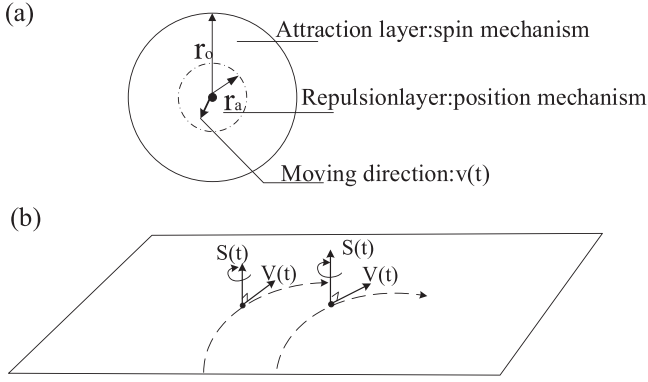
FIG. 1. (a) The spin model with collision avoidance. (b) Two-dimensional schematic for the relation of spin, velocities, and trajectories of two particles.

As shown in Fig. 1, since collision avoidance has the highest priority here, particles are ensured to keep a preset minimum distance $r_a > 0$ between itself and its neighbors. Thus, the particle velocity evolves as follows:

$$\mathbf{v}_i(t + \Delta t) = \rho\{-\Sigma_{j \neq i}[\mathbf{x}_j(t) - \mathbf{x}_i(t)]\}. \tag{6}$$

If no neighbors appear inside the circle of radius r_a of a particle, then the particle will attract other ones in a larger circle with radius of $r_o > r_a$ according to the proposed spin model (4) and (5). Analogous to the Couzin model [2,36], within the repulsion zone r_a, the information is the particle position distance, preventing collisions between particles. Within the circle of orientation of radius r_o, the particles aligns the current velocity by the protocol (4).

Often, some individuals in natural biological groups have more information or are more dominant than others, such as safe migration routes and new food or water sources [37,38]. Therefore, it is assumed that a small number of members have a preferred direction $\mathbf{d}$ to somewhere whereas other followers do not. All particles only know their directional preferences, but they do not have knowledge about other particles' directional preferences. Bearing in mind the net influence of both its neighbor(s) $\mathcal{N}_i$ and its own direction preference $\mathbf{d}_i$, the final moving direction of particle i could be calculated by

$$\mathbf{v}_i(t + \Delta t) = \rho[\mathbf{v}_i(t) + w_i\mathbf{d}_i(t)] + \Delta\mathbf{v}_i(t), \tag{7}$$

where the weight $\omega_i \in [0, 1]$ and $\Delta\mathbf{v}_i$ is a Gaussian noise. By tuning ω, one can change the influence of a leader's preferred direction on the collective motion of the whole group. More precisely, $\omega = 0$ means that the direction $\mathbf{d}_i$ has no influence on the other particles, whereas $\omega > 0$ implies that it will influence the final direction decision. The closer the value of ω is to 1, the greater the influence of the particle's preference will be.

To characterize the quality of information transmission, a couple of order parameters are introduced.

First, the average velocity ϕ of all particles is defined as a group synchronization order parameter,

$$\phi = \frac{1}{Nv_0}\left|\Sigma_{i=1}^N \mathbf{v}_i\right|, \tag{8}$$

where $\phi = 0$ means that the particles move randomly; conversely, $\phi = 1$ implies that the whole group is in the same order, so all particles move in the same direction. Note that the synchronization order parameter ϕ only considers the followers.

Denote the instant center $\mathbf{c}(t)$ of the group by [25]

$$\mathbf{c}(t) = \frac{1}{N}\Sigma_{i=1}^N\mathbf{x}_i(t). \tag{9}$$

Then, the final collective direction $\mathbf{d}$ is calculated by $\mathbf{d} = \mathbf{c}(T_f\Delta t) - \mathbf{c}[(T_f - \overline{T})\Delta t]$, where $\overline{T}$ denotes the time interval under consideration, and T_f denotes the total number of the running steps. Meanwhile, the standard deviation σ is used here to evaluate the degree of dispersion of data,

$$\sigma = \left[\frac{1}{n-1}\sum_{i=1}^n(x_i - \bar{x})^2\right]^{1/2}. \tag{10}$$

Define a collection $\mathcal{S} := \mathcal{S}_1 \cup S_2$ with $\mathcal{S}_1 = \{x| -90° \leqslant x < 90°\}$ and $\mathcal{S}_2 = \{x|90° \leqslant x < 270°\}$. Calculate the standard deviations σ_1 and σ_2 of the sets $\mathcal{S}_1$ and $\mathcal{S}_2$, respectively, and then $\sigma_\mathbf{d} := (\sigma_1 + \sigma_2)/2$ would be used to represent the concentrating tendency of preferred direction.

III. SIMULATION AND ANALYSIS

In the spin models (5)–(7), a damping term related to spin is included, which reveals the direction information dissipation of the starling group [34,35]. With an increasing proportion of leaders and with different damping coefficients see Table I, the convergence of the group in switching motion is a challenging issue. To analyze it, the consensus state order ϕ is adopted to quantify the information dissemination procedure about the group direction.

When some leader clusters disagree about the preferred direction, the followers need to decide which direction to move along. The order parameter of the group direction $\Delta\mathbf{c}(\overline{T})$ is used as their final choice. In numerical simulations, both the proportion and the direction of distinct leader clusters

TABLE I. Model parameters

Parameter	Unit	Symbol	Values explored
Number of particles	None	N	40–600
Zone of repulsion	Unit	r_a	0 and 1
Zone of orientation	Unit	r_o	0–15
Sampling time	Second	Δt	0.1
Moment of inertia	Unit	χ	0.1–10
Strength of the alignment	Unit	J	0 and 1
Damping coefficient	Unit	η	0–100
Speed	Units	v_0	0.1–5
Greatest turning rate	Degree	θ	20–90
Weighting factor	None	ω	0 and 1
Proportion of leaders	None	p	0 and 1

Unit denotes the nondimensionality of the parameters in the model. Their characteristic length scales are related to the specific organism under study, e.g., the value of r_a for insects is smaller than that for mammal herds.
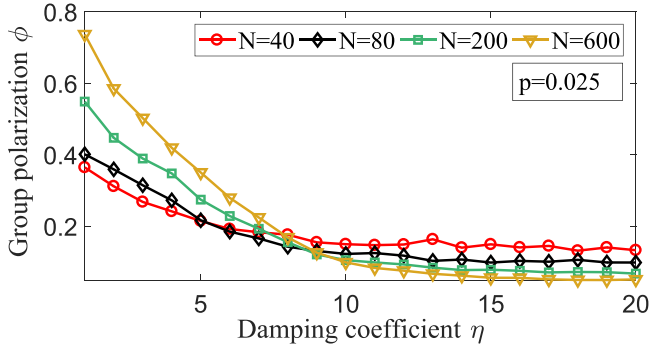
FIG. 2. The evolution of group polarization ϕ along increasing damping coefficient η for different sizes N of the group.

are changed, to reveal how group information transmission influences the collective decision making of the group.

Specifically, consider a group of N particles with random initial directions, zero initial spins $\mathbf{s}_i$ and sufficiently low external noise. Randomly pick a certain proportion p of particles as the leaders with an identical preferred direction $\mathbf{d}$. Other parameters: $\chi = 1.25$, $J = 0.8$, $r_a = 0.5$, $r_o = 2$, $\omega = 0.4$, $v_0 = 0.4$, $\Delta t = 0.1$, $\overline{T} = 50$, and $T_f = 5000$, maximum one-step tunable angle $\theta = 60°$.

Significantly, the directional change in the leaders affects the spin kinetics of the nearby particles, leading to a directional switch of the whole group. As can be observed from Fig. 2, the group polarization ϕ drops along ascending damping coefficient η. Another interesting phenomenon is observed in Fig. 3: the group polarization ϕ increases with rising proportion of the leaders, which implies that adding more leaders helps weaken the adverse influence of damping coefficient η. Moreover, the larger the group, the lower the proportion of the
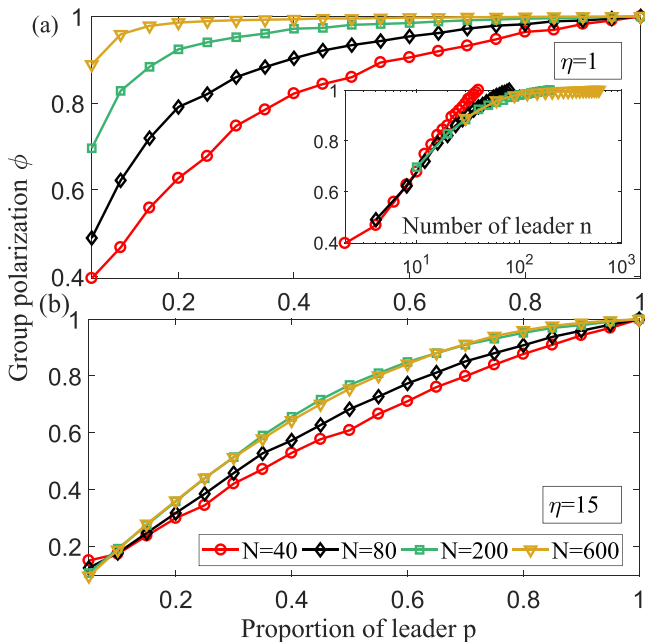
FIG. 3. The evolution of group polarization ϕ along increasing proportion p under different damping coefficients [$\eta = 1$ in panel (a) and $\eta = 15$ in panel (b)] and with different sizes N of the group.

Direction deviation $\mathbf{\Delta d}$ between divergent leader clusters(degrees)
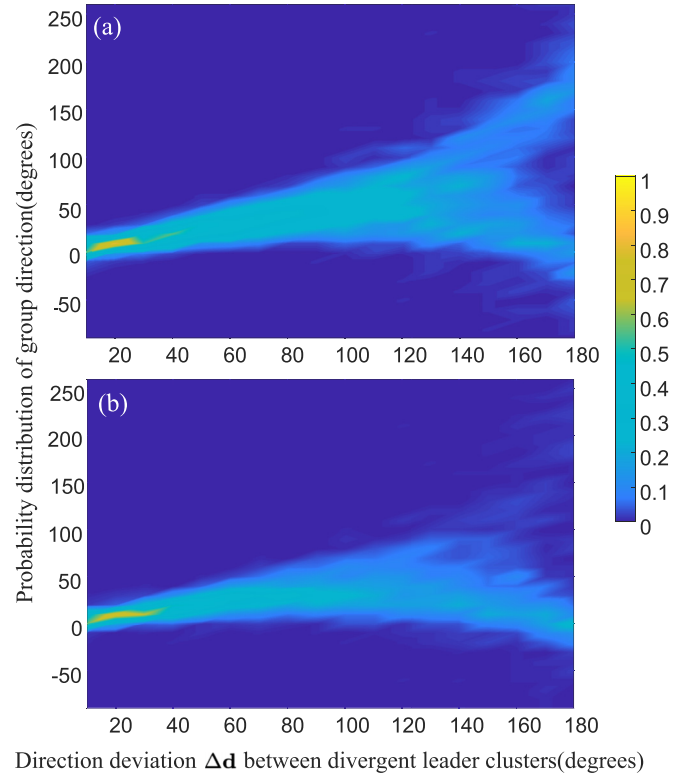
FIG. 4. Probability distribution for collective selection of group direction $\Delta \mathbf{c}(\overline{T})$ of two divergent leader clusters $\mathcal{L}_1$ and $\mathcal{L}_2$. Panels (a) and (b) illustrate the scenarios of balanced ($|\mathcal{L}_1| = |\mathcal{L}_2| = 10$) and unbalanced ($|\mathcal{L}_1| = 12$, $|\mathcal{L}_2| = 8$) leader clusters. Here, the divergent self-preferred moving directions $\Delta \mathbf{d} := \mathbf{d}_2 - \mathbf{d}_1$.

leaders is required to attain moving direction consensus as can shown in the inset of Fig. 3(a). Still, the leader proportion p needs to be increased to compensate the larger damping η. In Figs. 2 and 3, each point is an average over 200 independent runs.

However, the opinions of the leaders could not be always identical, and it often happens that different clusters of leaders have distinct preferred directions due to their own attractions or motivations. So, a new interesting question naturally emerges: What is the impact of leaders' divergence on collective decision making of the mass followers? In other words, which direction will the followers obey with increasing divergence of the two different leader clusters? To understand this, extensive numerical simulations have been conducted on the dynamic model (5)–(7) by tuning two key parameters, i.e., the preferred direction and the proportion of leaders.

More precisely, as shown in Fig. 4, consider two sets of randomly selected leader clusters $\mathcal{L}_1$ and $\mathcal{L}_2$. Parameters: $N = 100$, $\eta = 1$, $\mathbf{d}_1 = 0°$, and $\mathbf{d}_2 \in [0, 180]°$ with $10°$ intervals, $|\mathcal{L}_1| = |\mathcal{L}_2| = 10$ [panel (a)], $|\mathcal{L}_1| = 12$, $|\mathcal{L}_2| = 8$ [panel (b)]. Other parameters are the same as Fig. 3. In Fig. 4, each point is an average over 200 independent runs.

As shown in Fig. 4(a), a fascinating phenomenon is observed that the group direction undergoes a transition from a compromising phase (i.e., following the average) to a preferred phase (i.e., completely aligning to one leader cluster) when the directional divergence $\Delta \mathbf{d} := \mathbf{d}_2 - \mathbf{d}_1$ surpasses a
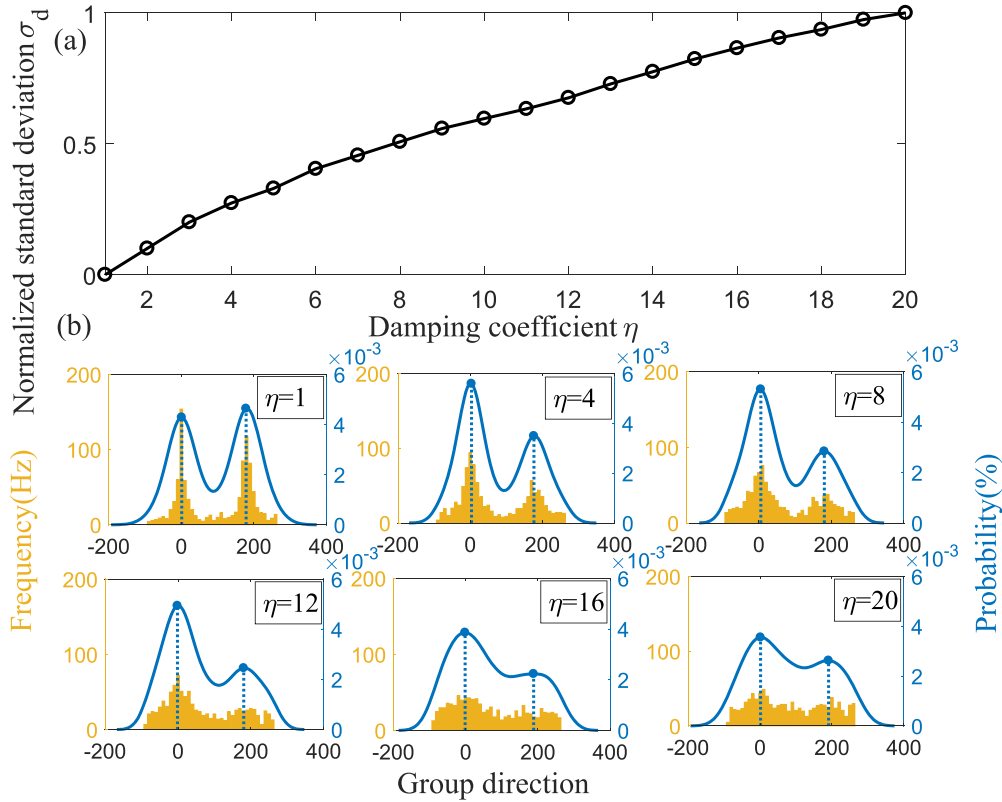
FIG. 5. Collective direction distribution when the divergence $\Delta \mathbf{d}$ of the two leader clusters has reached 180°. Here, $|\mathcal{L}_1| = |\mathcal{L}_2| = 10$). (a) The evolution of normalized standard deviation $\sigma_{\mathbf{d}}$ of the collective moving direction $\mathbf{d}$ with increasing damping coefficient η. (b) Distribution of the group directions with increasing values of η.

threshold $\overline{\mathbf{d}}$ about 120°. As shown in Fig. 4(b), it is found that the probability of preferred direction depends on the sizes of the two leader clusters as well. Since $|\mathcal{L}_1| > |\mathcal{L}_2|$, most of the followers select the larger leader cluster $|\mathcal{L}_1|$ in the preferred phase, which implies that a larger leader cluster has a greater influence on the followers. Counterintuitively, the transition point is always around 120°, regardless of the two leader clusters being identical or not.

Now, another concern is what role the damping coefficient plays in such a transition. Let the divergent preferred directions $\Delta d = 180°$. Here, a kernel density estimation method [39] is used to calculate the probability densities illustrating the distribution of the group directions over 1000 independent runs. Figure 5(a) shows that the normalized standard deviation $\sigma_{\mathbf{d}}$ of the collective moving direction $\mathbf{d}$ rises with ascending damping coefficient η, which implies that large η favors the fading of the directional concentrating effect. In Fig. 5(b), the two peaks of the curves denote the emergence of bistable states of the self-propelled particle system, which represents the most likely collective directions $\mathbf{d}$. It is observed that the double-peak phenomenon (or the bistable state) fades away, and the compromising tendency is thereby intensified with increasing damping coefficient η.

IV. CONCLUSION

This paper investigates the moving direction decision-making mechanism of self-propelled spin particle systems. Inspired by the work of Attanasi *et al.* [34] and Cavagna *et al.* [35], we have established an inertial spin model. Through extensive numerical simulations, it is revealed that the moving direction of a group of self-propelled spin particles undergoes a transition from a compromising phase to a preferred phase by tweaking the divergence of the preferable moving directions of two leader clusters. Interestingly, the larger damping effect of the moving direction helps attenuate the preference-switching transition phenomenon. This paper can be expected to help pave the way from collective motion dynamics theory to formation control or regulation applications of multiagent systems, such as multiple unmanned systems, manufacturing robot swarms, wireless sensor networks, and so on.

[1] C. W. Reynolds, SIGGRAPH Comput. Graph. **21**, 25 (1987).

[2] I. Couzin, J. Krause, R. James, G. Ruxton, and N. Franks, J. Theor. Biol. **218**, 1 (2002).

[3] T. Vicsek, A. Czirók, E. Ben-Jacob, I. Cohen, and O. Shochet, Phys. Rev. Lett. **75**, 1226 (1995).

[4] F. Ginelli and H. Chaté, Phys. Rev. Lett. **105**, 168103 (2010).

[5] M. R. D'Orsogna, Y. L. Chuang, A. L. Bertozzi, and L. S. Chayes, Phys. Rev. Lett. **96**, 104302 (2006).

[6] J. Buhl, D. Sumpter, I. Couzin, J. J. Hale, E. Despland, E. R. Miller, and S. Simpson, Science **312**, 1402 (2006).

[7] Z. Chen and H. T. Zhang, Automatica **49**, 1236 (2013).

[8] H. Tanner, A. Jadbabaie, and George J. Pappas, IEEE Trans. Autom. Control **52**, 863 (2007).

[9] A. Flack, M. Nagy, W. Fiedler, I. Couzin, and M. Wikelski, Science **360**, 911 (2018).

[10] D. Chen, T. Vicsek, X. Liu, T. Zhou, and H. T. Zhang, Europhys. Lett. **114**, 60008 (2016).

[11] H. Barbosa, M. Barthelemy, G. Ghoshal, C. James, M. Lenormand, T. Louail, R. Menezes, J. J. Ramasco, F. Simini, and M. Tomasini, Phys. Rep. **734**, 1 (2018).

[12] D. Helbing, I. Farkas, and T. Vicsek, Nature (London) **407**, 487 (2000).

[13] C. Becco, N. Vandewalle, J. Delcourt, and P. Poncin, Physica A **367**, 487 (2006).

[14] M. Davis and B. L. Olla, Environ. Biol. Fishes **34**, 421 (1992).

[15] A. Garcimartín, and J. M. Pastor, and L. M. Ferrer, and J. J. Ramos, and C. Martín-Gómez, and I. Zuriguel, Phys. Rev. E **91**, 022808 (2015).

[16] A. Szabó, R. Mayor, Curr. Opin. Cell Biol. **42**, 22 (2016).

[17] S. Henkes, K. Kostanjevec, JM. Collinson, R. Sknepnek, and E. Bertin, Nat. Commun. **11**, 1405 (2020).

[18] S. Martínez, J. Cortés, and F. Bullo, IEEE Contr. Syst. Mag. **27**, 75 (2007).

[19] I. Akyildiz, W. Su, Y. Sankarasubramaniam, and E. Cayirci, Comput. Networks **38**, 393 (2002).

[20] I. Slavkov, D. Carrillo-Zapata, N. Carranza, X. Diego, F. Jansson, J. Kaandorp, S. Hauert, and J. Sharpe, Sci. Robot. **3**, eaau9178 (2018).

[21] R. Olfati-Saber, IEEE Trans. Autom. Control **51**, 401 (2006).

[22] L. Caprini and U. Marini Bettolo Marconi, and A. Puglisi, Phys. Rev. Lett. **124**, 078001 (2020).

[23] L. Caprini, U. Marini Bettolo Marconi, C. Maggi, M. Paoluzzi, and A. Puglisi, Phys. Rev. Research **2**, 023321 (2020).

[24] K. Singh and Y. Rabin, Sci. Rep. **9**, 17910 (2019).

[25] T. Vicsek and A. Zafeiris, Phys. Rep. **517**, 71 (2012).

[26] F. Cucker and S. Smale, IEEE Trans. Autom. Control **52**, 852 (2007).

[27] L. Caprini and U. M. B. Marconi, Soft Matter **17**, 4109 (2021).

[28] G. Szamel and E. Flenner, Europhys. Lett. **133**, 60002 (2021).

[29] Z. Cheng, Z. Chen, T. Vicsek, D. Chen, and H. T. Zhang, New J. Phys. **18**, 103005 (2016).

[30] H. T. Zhang, M. Chen, and T. Zhou, Europhys. Lett. **86**, 40011 (2009).

[31] Z. Chen, H. T. Zhang, X. Chen, D. Chen, and T. Zhou, Europhys. Lett. **112**, 20008 (2015).

[32] H. T. Zhang, M. Z. Q. Chen, T. Zhou, and G. Stan, Europhys. Lett. **83**, 40003 (2008).

[33] M. Nagy, Z. Akos, D. Biro, and T. Vicsek, Nature (London) **464**, 890 (2010).

[34] A. Attanasi, A. Cavagna, L. Del Castello, I. Giardina, T. Grigera, A. Jelic, S. Melillo, L. Parisi, O. Pohl, E. Shen, and M. Viale, Nat. Phys. **10**, 691 (2014).

[35] A. Cavagna, L. Castello, I. Giardina, T. Grigera, A. Jelic, S. Melillo, T. Mora, L. Parisi, E. Silvestri, M. Viale, and A. Walczak, J. Stat. Phys. **158**, 601 (2015).

[36] I. Couzin, J. Krause, N. Franks, and S. Levin, Nature (London) **433**, 513 (2005).

[37] S. G. Reebs, Anim. Behav. **59**, 403 (2000).

[38] M. Lindauer, Nature (London) **179**, 63 (1957).

[39] E. Parzen, Ann. Math. Statist. **33**, 1065 (1962).